2024 NDIA MICHIGAN CHAPTER
GROUND VEHICLE SYSTEMS ENGINEERING
AND TECHNOLOGY SYMPOSIUM
POWER & MOBILITY TECHNICAL SESSION
AUGUST 13-15, 2024 - NOVI, MICHIGAN

On-Board Fuel Sensing for UAS and Ground Vehicle Applications

Dev B. Patel[1], Ashish Sutar[1], Abhinav Abraham[1], Dhananjay Ambre[1], Haruna Okada[2], Jacob M. Stafford[2], Niranjan Miganakallu[2], Eric Mayhew[3], Kenneth S. Kim[3], Scott Sanders[2], David Rothamer[2], Kenneth Brezinsky[1], Patrick T. Lynch[1]

[1] Department of Mechanical and Industrial Engineering, University of Illinois Chicago, Chicago, IL
[2]Department of Mechanical Engineering, University of Wisconsin-Madison, Madison, WI
[3]US Army Combat Capabilities Development Command, Army Research Laboratory, Aberdeen Proving Ground, MD

ABSTRACT

The variability in fuel, particularly for fuel blends containing sustainable aviation fuels (SAFs), emphasizes the importance of understanding fuel properties for optimizing engine performance. This paper introduces spectroscopic fuel sensors capable of real-time estimation of jet fuel properties, mainly derived cetane number (DCN). While initially developed for unmanned aircraft systems (UAS), the paper explores their potential in ground vehicle applications: enhancing engine performance through sensing for feed-forward control and fuel property monitoring at fuel depots. The fuel sensing technologies are based on spectroscopic techniques coupled with machine learning (ML) approaches. The combination of these techniques demonstrates a promising solution for a wide spectrum of fuel applications.

Citation: D. Patel, A. Sutar, A. Abraham, D. Ambre, H. Okada, J. Stafford, N. Miganakallu, E. Mayhew, K. Kim, S. Sanders, D. Rothamer, K. Brezinsky, P. Lynch, "*On-Board Fuel Sensing for UAS and Ground Vehicle Applications*" In *Proceedings of the Ground Vehicle Systems Engineering and Technology Symposium* (GVSETS), NDIA, Novi, MI, Aug. 13-15, 2024.

1. INTRODUCTION

Internal combustion engines (ICEs) play a significant role in the propulsion systems of ground vehicles and small to mid-sized aircraft. Traditionally, these engines have relied on conventional fuels such as gasoline, diesel, and jet fuels. To mitigate logistical challenges associated with the supply chain of using multiple fuels for various ground vehicles and aircraft, the Department of Defense (DoD) implemented a 'Single Fuel Policy.' Under this policy, JP-8 was chosen as the primary fuel, meeting the requirements of the United States military for both ground vehicles and aircraft [1]. Subsequently, F-24

was incorporated due to its close resemblance to JP-8, providing a standardized approach for fuel usage within the military [1, 2].

In response to environmental and sustainability concerns, there has been increased interest in the use of alternative fuels, including biodiesel, renewable diesel, ethanol, and sustainable aviation fuels (SAFs). However, characteristics of these fuels, driven by fuel properties such as density, calorific value, aromatic content, enthalpy of vaporization, and cetane number (CN) or derived cetane number (DCN), can vary widely between these fuels and their conventional counterparts [3]. This is particularly true for SAFs where CNs are known to vary from as low as 15 to greater than 50 [4]. Notably, conventional jet fuels exhibit variations in properties as well [5]. When using fuels with wide-ranging ignition properties in compression-ignition (CI) ICEs, measuring the fuel's ignition properties coupled with engine combustion control can account for variations in fuel properties.

1.1. Variability of Fuel and Blends

As mentioned above, the use of conventional and sustainable fuel blends has increased, and the Department of Energy (DoE) developed a roadmap for SAFs in 2022 and identified nine SAF production pathways that have met the qualification criteria outlined in ASTM D4054 and ASTM D7566. This qualification allows for the blending of alternative fuels with conventional fuels [6]. The DCNs of SAFs are more diverse than conventional jet fuels, with Fischer-Tropsch Synthetic Paraffinic Kerosene (FT-SPK) fuel having a DCN of 60 and iso-butanol-derived alcohol-to-jet (ATJ) fuel having DCN of 15 [4].

Hydrocarbon molecular families, including n-alkanes, iso-alkanes, cycloalkanes, and aromatics, determine the properties of conventional fuels and SAFs. Normal- and iso-alkanes are characterized by higher specific energy, but lower energy density compared to aromatics, which exhibit contrasting attributes [7]. By blending these hydrocarbon families in alternative jet fuels, blends can obtain fuel characteristics that are more suitable for ICEs.

1.2. Fuel Property Sensing for Aircraft

CI engines that can operate on these jet fuel blends with a wide range of properties offer potential as a propulsion system for unmanned aircraft systems (UAS). As SAFs and blends become integrated into commercial and military applications, the need to monitor fuel properties before and during operation has increased. An on-board fuel sensor coupled to an adaptive engine control system with sufficient mechanisms for ignition enhancement would allow for the operation of these UAS on a wider range of fuels and blends of fuels. For the engine control to adapt and optimize combustion, sensing properties of the fuel is critical. For CI engines, the most important fuel property is the ignition tendency of fuel, quantified by CN, which is associated with the ignition delay time (IDT). The IDT, defined as the duration from the start of injection (SOI) to the start of combustion (SOC), serves as a measure of the delay until combustion under elevated temperature and pressure conditions. A low CN (< 40) can result in engine misfires due to a long IDT. While a minimum CN specification is included for diesel fuel [8], there is no minimum CN specification for jet fuels. The standard process for determining CN/DCN involves the use of standard equipment like Cooperative Fuel Research (CFR) engines for CN (ASTM D613) [9] and Ignition Quality Testers (IQTs) or Fuel Ignition Testers (FITs) for DCN (ASTM D6890 and ASTM D7668, respectively) [10].

Conventional CN/DCN measurement devices are high accuracy but are also large, cumbersome to operate, and have high fuel

consumption requirements. These types of devices would be unsuitable for operation on small to medium-sized aircraft and ground vehicles. Alternatively, spectroscopic fuel sensors can allow for on-board real-time evaluation of jet fuel properties [3]. Several studies show that fuel properties can be correlated with the spectra of fuels with the use of Machine Learning (ML) to predict the fuel properties [11-14].

Spectroscopic fuel sensors coupled with feed-forward engine control could enable aircraft with ICEs to operate on a wider range of jet fuels. These sensors must be miniaturized and non-intrusive to allow for on-board deployment [3]. There are no commercial fuel system sensors currently available that are miniaturized and able to be integrated in-line with an engine. In this work we report and demonstrate three spectroscopic fuel sensor prototypes (shown in Fig. 1) capable of determining DCN. The three developed sensors employ spectroscopic techniques described in previous work [3], including dispersive near-infrared (NIR), Fourier transform – attenuated total reflectance (FT-ATR) absorption spectroscopy, and Raman scattering. The developed fuel sensor prototypes use modified commercially available spectrometers. The spectrometers exhibit variations in size, volume, weight, peak power load, and spectral measurement capabilities, such as the range and resolution.

The dispersive NIR sensor utilizes a commercially available FlameNIR spectrometer from Ocean Insight, as well as valves and a pump for obtaining a reference spectrum [3]. The dispersive NIR sensor is fully enclosed with external dimensions measuring at 24 x 15.25 x 14.6 centimeters resulting in a volume of about 6225 cm^3 and weighing approximately 3 kgs.

The FT-ATR sensor employs an ATR sampling technique for spectral acquisition. The benchtop FT-ATR spectrometer (Bruker Vertex 70) has dimensions of 84 x 65 x 30 centimeters with a total volume a little less than 147900 cm^3 and a weight of approximately 70 kgs.

The Raman sensor stands at 18.5 x 14.5 x 7.4 centimeters for a total volume of around 2500 cm^3 with a weight of approximately 1 kg. The Raman spectrometer used in this sensor was acquired from Wasatch Photonics.

All sensors can perform real-time spectral acquisition and simultaneously output a fuel property prediction with the use of single board processors or a computer. The frequency of property prediction is referred to as the response time of the sensor [3] which can be found in Table 1, along with a summary of other characteristics of the sensors. The spectral range indicated in Table 1 refers to the spectral range that each sensor is currently capable of measuring.

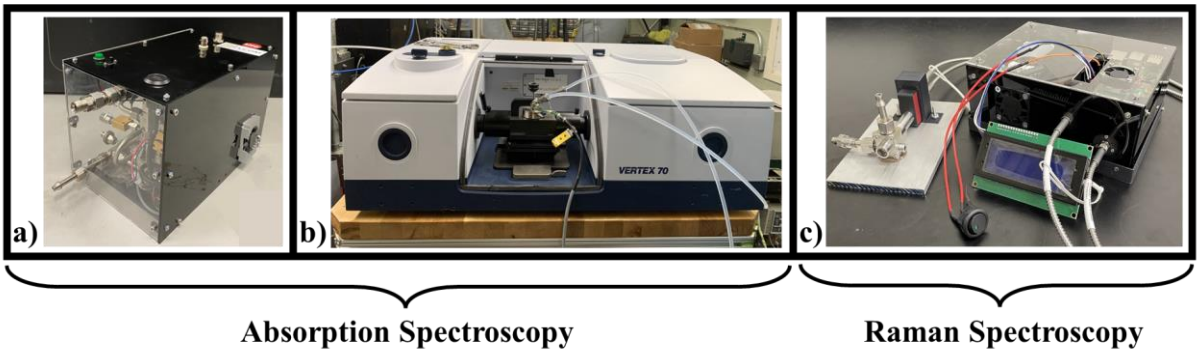

Figure 1. (a) Dispersive NIR Sensor, (b) FT-ATR Sensor, (c) Raman Sensor

Table 1. Current Spectroscopic Fuel Sensor Characteristics [3]

Fuel Sensor	**Units**	**Dispersive NIR**	**FT-ATR**	**Raman**
Volume	cm^3	6223	147844	2490
Weight	kg	3	70	1
Peak Power Load	W	9	180	8
Time Response	s	10	3	18
Spectral Range	cm^{-1} nm*	900-1700*	4000-400	1800-500 *(Raman shift from 785nm laser)*
Spectral Resolution	cm^{-1} nm*	10*	2	7

It should be noted that a sensor like the FT-ATR can have a higher resolution and broader spectral measurement but is not the most miniaturized. Pathways to further miniaturize the sensors are being investigated. The required spectral range and resolution will directly impact the size of the sensor [3].

Future work will reduce the size, weight, and power requirement (SWAP), while maintaining the desired prediction accuracy. The dispersive NIR sensor may reduce its SWAP to about 800 cm^3, 0.55 kg, and 3 W. The FT-ATR may be able to drastically reduce its size to less than 350 cm^3 with a weight of a little more than 0.5 kg, while having a power requirement of 12 W. Lastly, the Raman sensor will be able to reduce its volume to about 800 cm^3 and have a weight of a little more than 0.5 kg.

1.3. Applications to Ground Vehicles

Fuel sensing technology can be beneficial to the ground vehicle community as CI engines are employed on many large ground vehicles. These engines were originally designed to operate on diesel fuels that exhibit certain fuel characteristics with one of the key requirements of having a CN greater than 40 [15]. The ability to monitor fuel properties on-board a vehicle can enable the engines to operate on a wide range of fuels and enable feed-forward engine control that accounts for fuel property variations. In colder climates, ground vehicles often have trouble at startup [1]. Feed-forward engine control with fuel ignition quality determined from an on-board fuel sensor could be used to adjust glow plug power and fuel injection timing [16, 17] to improve cold start process when using low CN fuels. This can aid in cold starts often experienced by CI engines and reduce emissions [18]. Feed-forward engine control with on-board fuel sensing could also increase fuel efficiency and the durability/lifespan of the engine [18]. The use of a spectroscopic fuel sensor shows a promising solution for real-time, on-board evaluation of fuel properties. This can enable optimal engine performance by implementing feed-forward engine control with fuel sensing.

Currently, fuel monitoring to check compliance with ASTM standards requires human intervention and is not a non-destructive approach [19]. A combination of chromatography and spectroscopic techniques are used to identify and quantify hydrocarbon classes in gasoline, diesel, and kerosene and to determine fuel properties [19]. Spectroscopic techniques are already being used to monitor fuel composition using lab grade equipment. These lab grade devices that require sample extraction can be replaced with an inline sensor to passively monitor fuel properties real-time without requiring human intervention.

In the subsequent sections, we present the process used to create the dataset to train accurate ML models for fuel property prediction, highlighting the existing work on jet fuels and near jet fuels for DCN. Next, we

discuss the integration of spectroscopic fuel sensors in line with a CI engine and demonstrate real-time fuel property measurement capabilities, one possible scenario for ground vehicle applications. Future work will also be discussed to show next steps in developing a more versatile spectroscopic fuel sensor for ground vehicle applications.

2. ACCURATE TRAINING SETS FOR BROADER RANGE OF FUELS

Developing a fuel property sensor capable of accurately predicting the diverse physiochemical properties of petroleum-based fuels, including SAFs, presents a significant challenge. These fuels exhibit considerable variability in their physiochemical properties owing to their complex compositions which include various hydrocarbons, additives, stabilizers, etc. Achieving reliable predictions requires a comprehensive training dataset that encompasses a variety of functional groups present in these fuels. Only then can models be effectively trained to accurately predict the diverse range of properties exhibited by these fuels.

2.1. Approach for Representing Jet Fuels

Constructing robust models for fuel property prediction requires a comprehensive training dataset. However, training ML models on every available fuel is impractical and may introduce bias toward the fuels in the dataset. To address this challenge, Mehta et al. used approximately 17 real fuels and complex CN fuel surrogates provided by the Army Research Laboratory (ARL) to build a dataset [20]. The study employed two-dimensional gas chromatography (GCxGC) coupled with flame ionization detector (FID) and time of flight-mass spectrometry (TOF-MS) analysis to characterize the fuels. The components were classified into family/size-based categories, and a chemical functional group fragmenter was applied to suggest the ranges of UNIFAC chemical functional groups present in these fuels.

Using these UNIFAC functional groups, the DCN, molecular weights of these real fuels, and a selection of pure hydrocarbons, Sheyyab et al. [21] developed a chemical functional group optimizer (CFGO). This optimizer used the aforementioned information and produced mixtures or fuel surrogates (which included up to four pure components) that spanned and encompassed the range of UNIFAC chemical functional groups, DCNs and molecular weights of real fuels. The initial dataset comprised 23 pure components and 79 mixtures [12, 21]. Hydrocarbon mixtures were prepared in-house using these components. The weight fractions of all pure components to make surrogates for the entire dataset were determined using the CFGO.

As discussed, the DCN is extremely important in CI engines and the focus of work described here. The DCN measurements were conducted in-house using an IQT following ASTM D6890-18 standards for all mixtures, fuels, selected blends, and most neat hydrocarbons (DCN>15). For pure hydrocarbons not measured in an IQT, DCNs were obtained from the literature [22].

2.2. Use of ML Models to Correlate Spectra to DCN

Fuel properties can be correlated with the spectral information of fuel, leading to ML approaches in numerous studies to predict these properties [3]. Spectroscopic techniques such as dispersive NIR, FT-ATR, and Raman spectroscopy, operating at different wavelength ranges and resolutions, have been employed to develop ML models correlating to DCN [11-14]. Linear and non-linear models were used including but not limited to multi linear regression (MLR), support vector regression (SVR), lasso

regression, random forest regression, etc. All models were employed in Python using scikit-learn module [23].

2.3. Jet Fuels Dataset

The models were trained on the dataset comprising some jet fuels and the mixtures of pure components as discussed in the previous section. The prediction performances of the models have been evaluated using a testing set of jet fuels, SAF, and blends of jet fuels, assessing the DCN prediction performance of different linear and non-linear ML models trained on the training set [11, 12, 21]. Table 2 shows the training and testing split for the ML models to make DCN predictions. The split ensured that complex non-linear blending of DCN was taken into consideration.

2.4. Results (DCN Accuracy):

The spectroscopic techniques (mentioned in Section 1.2) underwent training and testing using the dataset shown in Table 2. Table 3 showcases the model performance for the different sensors and sensing techniques [12, 13]. All methods demonstrate a strong capability to predict DCN for the samples in the test set, with R^2 scores consistently surpassing 0.86, indicative of good fits. Additionally, nearly all samples in the testing set fall within the 10% error limit.

In the NIR region, the C-H first overtone around 6250 cm^{-1} and the C-H combination band around 7142 cm^{-1} were found to play significant roles in DCN prediction. Conversely, in the IR region, the asymmetric CH_2 and CH_3 stretch around 3000 cm^{-1}, the aromatic C-H bend around 1000 cm^{-1} , and C-H second overtone around 833 cm^{-1} were identified as important features [11, 13].

The FT-ATR study highlights the significance of CH_3, CH_2, and aromatic functional groups in DCN prediction. Dispersive NIR analysis also yields satisfactory results. FT-ATR emerges with the lowest Mean Percentage Error (MPE) and

Table 2. Training and testing dataset for generating ML models

Name, description, or POSF (as applicable)	**DCN**
TRAINING	
79 mixtures made using 23 neat hydrocarbons	15– 78.5
ARL-CN30	34.70
ARL-CN35	36.70
ARL-CN40	41.90
ARL-CN45	49.70
ARL-CN50	55.09
ARL-CN55	59.50
F-24	46.59
ATJ – POSF11498	15.89
JP-10**	18.85
RP-2 – POSF5433**	51.26
RP-2 – POSF7688**	51.29
TESTING	
JetA1 – POSF10264	49.29
JetA2 – POSF10325	49.00
JetA3 – POSF10289 (JP5)	40.20
50/50 wt % ARL – CN35/CN55*	49.59
50/50 wt % ARL – CN35/CN45*	43.00
50/50 wt % ARL – CN30/CN50	45.09
50/50 wt % ARL – CN45/CN55	54.68
50/50 wt % ARL – CN35/CN40	39.79
50/50 wt % F-24/ATJ	34.59
30/70 wt % F-24/ATJ	29.60
70/30 wt % F-24/ATJ	39.50
20/80 wt % F-24/ATJ*	28.29
40/60 wt % F-24/ATJ	34.00
60/40 wt % F-24/ATJ	39.09
80/20 wt % F-24/ATJ	43.40
50/50 wt % JP10/ARL – CN55**	44.09
50/50 wt % JP10/F-24**	35.29
50/7.5/42.5 wt % JP10/ARL – CN55/F-24**	37.59
80/20 wt % CN35/CN55**	43.43
20/80 wt % CN35/CN55**	55.53
28/72 wt % CN30/CN45**	46.24
30/70 wt % CN40/CN50**	52.18
37.45/62.55 wt % CN40/CN55**	53.77
70/30 wt % CN30/CN35**	35.61
41.5/58.5 wt % CN30/CN35**	35.80
41.5/58.5 wt % CN40/CN45**	47.00
42/28.4/29.6 wt % CN30/CN55/F-24**	47.45
60/40 wt % CN30/CN40**	38.17
50/50 wt % CN30/F-24**	41.40
50/50 wt % CN45/F-24**	48.90
57/43 wt % CN30/CN40**	37.88
25/75 wt % CN55/F-24**	50.72
22/31/47 wt % CN40/CN50/F-24 **	50.28
65/35 wt % F-24/ATJ**	39.38
55/45 wt % F-24/ATJ**	36.73
50.5/49.5 wt % F-24/ATJ**	35.54

* Used only with Dispersive NIR and ATR models
** Used only with Raman models

tied with Raman spectroscopy for highest R^2 score among all techniques.

Table 3. Performance of ML models

Spectroscopic Technique	Spectral Range (cm^{-1})	R^2 Score	MPE (%)	% of samples within ±10% error
Dispersive NIR	10500-6056	0.86	5	97
FTIR-ATR	3200-800	0.89	4.58	95
Raman	1800-500 *(Raman shift from 785nm laser)*	0.89	4.69	93.33

3. FUEL SENSING DEMONSTRATION

To demonstrate the real-time fuel property measurement capabilities, the three sensors—utilizing different spectroscopic techniques employing the ML models described in Section 2—were integrated into a CI engine test cell at the University of Wisconsin – Madison. The sensors were evaluated for their ability to determine the DCN of the engine-supply fuel, which was intentionally varied over time by switching between two fuels with different DCN. To assess the adaptability of the ML models, one of the fuels was used for training the machine learning models, while the other one was not. The predictions made by the sensors were validated by collecting samples of the fuel being supplied to the engine during the test and measuring their DCN experimentally using the ASTM D6890 method at the University of Illinois Chicago.

3.1. Experimental Setup

The experimental engine test cell employed in the demonstration featured a production 2.0-L 4-cylinder diesel engine (GM 2.0-L A20DTH) that had been modified for single-cylinder, energy-assisted compression-ignition (EACI) engine operation. A more detailed description of the engine setup can be found in the provided references [24-26]. Figure 2 shows a schematic of the fuel system utilized during the demonstration, with the three sensors shown in Figure 1.

This fuel system consisted of two fuel tanks, each equipped with its own lift pump and flow regulator. A 3-way diverting valve was used to switch between these two tanks during the fuel switch experiments. Following the diverting valve, the fuel passed through all three fuel sensors in series. The

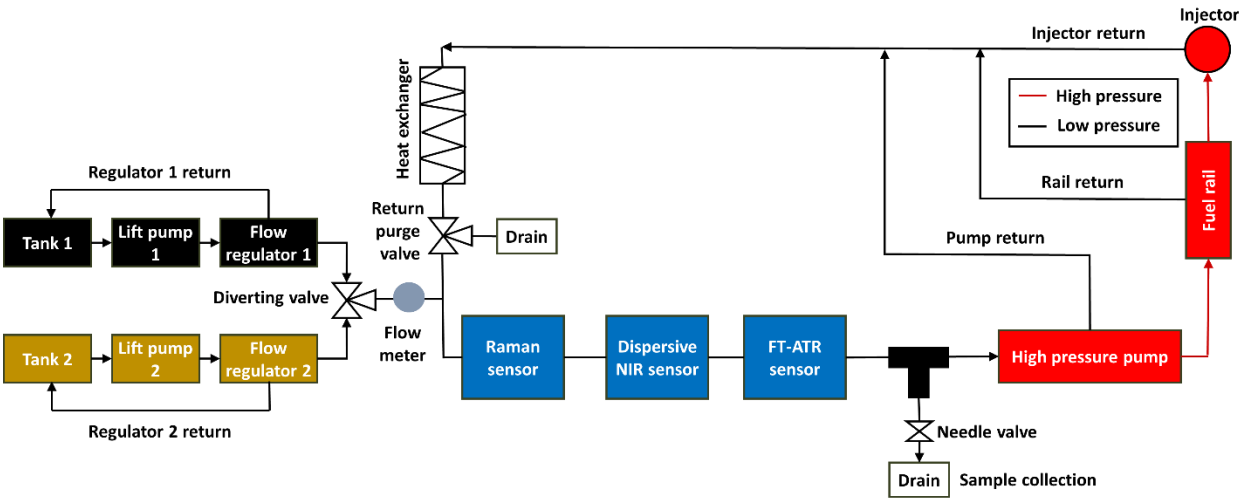

Figure 2. Schematic of experimental fuel system with fuel sensor integration

typical temperature and pressure at the inlet of the first fuel sensor were 15°C and 103.4 kPag, respectively.

Downstream of the sensors, a tee fitting (shown in black) was installed, with one leg connected to a needle valve and a drain container. This valve allowed for sampling of fuel during the fuel switching experiments for later IQT testing. Following the tee, the fuel entered the high-pressure pump (Bosch CP3), which operated at a constant speed via a DC motor. To maintain steady operating conditions, fuel returns from the pump, rail, and injector were directed through a heat exchanger to cool the fuel before returning to the system. The return purge valve after the heat exchanger normally directed all fuel returns to the system. However, when removal of return fuel was required, the return purge valve directed the fuel to the drain.

The fuel switching experiment was conducted using ATJ and F24 (Jet-A with military additives). The upper limit DCN fuel employed in this demonstration consisted of 100 vol. % F24 with a DCN of 46.59. The lower limit DCN fuel utilized was comprised 40 vol. % F24, with the remaining balance being ATJ, resulting in a blend DCN of 34. The upper limit DCN and lower limit DCN fuels will be referred to as DCN46 and DCN34 fuels, respectively. Detailed properties of each fuel and the blend can be found in Table 4. While the DCN46 fuel was included in the training set of the ML models, the DCN34 was not.

Table 4. Fuel property information: derived cetane number (DCN), lower heating value (LHV), density @ 288 K (ρ), kinematic viscosity @ 313 K (ν), and temperature of 10% (T10), 50% (T50), and 90% (T90) recovered volume for ASTM D86.

Property	Units	F24	40% F-24/ 60% ATJ	ATJ
DCN*	-	46.59	34	17.42
LHV	MJ/kg	43.1	43.7	43.9
ρ @ 288 [K]	kg/m^3	803.7	777	761
ν @ 313 [K]	mm^2/s	1.377	1.446	1.53
Aromatics	% vol.	15.4	6.3	<0.01
Olefins	% vol.	1.2	1.4	0
Saturates	% vol.	83.4	92.4	99.62
T10**	°C	176.5	177	178.9
T50**	°C	207.7	189.8	183.3
T90**	°C	250.6	241	224.4
*ASTM D6890 ** ASTM D86				

3.2. Results

In this demonstration, the fuel supply underwent three switches between the DCN34 and DCN46 fuels. Initially, the engine ran on DCN34 fuel, followed by switches to DCN46, back to DCN34 and finally to DCN46 fuel. During the last transition from DCN34 to DCN46 fuel, six fuel samples were collected and later measured for their DCN using an IQT. Figure 3 illustrates the temporal evolution of DCN estimates from the fuel sensors alongside the DCN values from the IQT measurements.

Initially, the DCN predictions from all the sensors were around 33, aligning with the DCN of the fuel. Upon switching to DCN46 fuel, a period of fuel mixing occurred within the system due to the unconsumed fuel returning and recirculating. Over time, the DCN predictions gradually increased from 33 to 46, reflecting this mixing process. Around the 2000-second mark, the DCN predictions stabilized at approximately 46. Although there were slight discrepancies between the predictions from the dispersive NIR sensor and those from the Raman and FT-ATR sensors, all predictions were within the 10% error margin specification, as anticipated from the assessment of the DCN accuracy of the ML models detailed in Section 2.

Once the DCN predictions stabilized at around the 2000-second mark, the fuel supply was switched back to DCN34, the fuel injection was paused, and the rail pressure was decreased. The return purge valve after

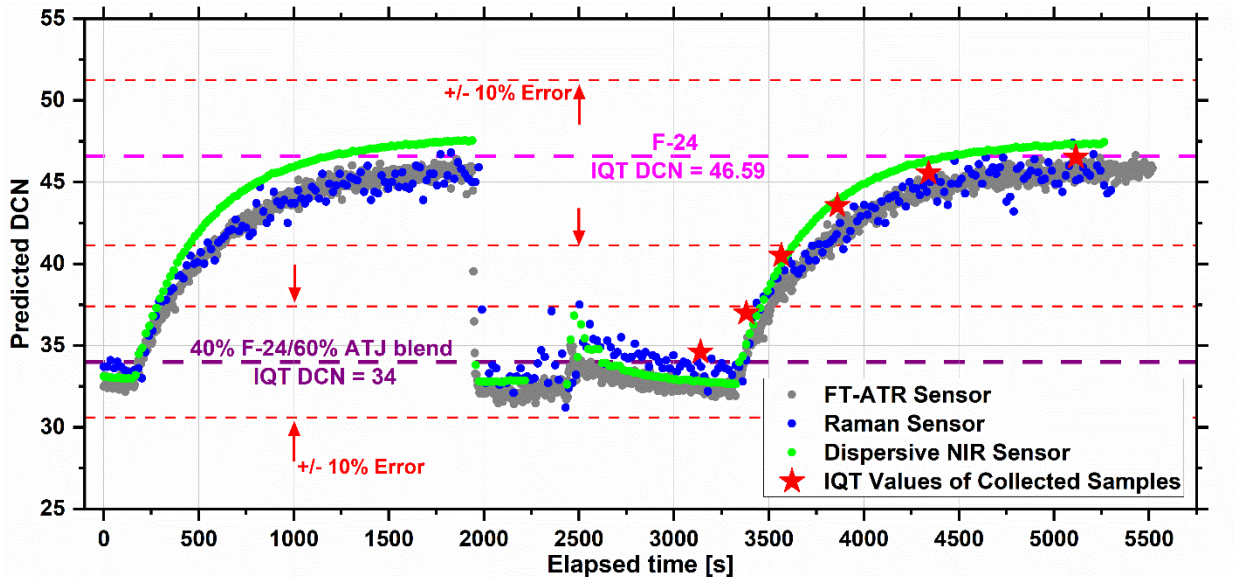

Figure 3. DCN predictions from the fuel sensors and the IQT measurements

Table 5. Percentage errors of the DCN predictions, as provided by the sensors, when compared to the IQT measurements

Sensor	Percent error [%]						Average absolute percent error [%]
	Sample 1	Sample 2	Sample 3	Sample 4	Sample 5	Sample 6	
Dispersive NIR	-5.21	-1.90	0.38	1.40	2.10	1.73	2.12
Raman	-4.11	0.50	-1.32	-4.40	-1.63	-2.05	2.34
FT-ATR	-6.12	-2.97	-4.04	-2.74	-1.80	-1.92	3.27

the heat exchanger then directed all fuel returns to the drain to quickly remove the remaining DCN46 fuel in the fuel system, resulting in a rapid decline in DCN predictions. At around 2500 seconds, the drain valve was closed, and the rail pressure was increased again. The slight rise in DCN predictions is likely due to residue of DCN46 fuel remaining in the rail, which was pushed out and recirculated upon increasing rail pressure.

Around 500 seconds later, the fuel injection resumed while DCN predictions started to stabilize around 33. Subsequently, at 3300 seconds, the fuel supply was switched back to the DCN46 fuel, causing DCN predictions to rise similarly to the initial switch. During this final fuel transition, fuel was collected at the drain after the tee in six 50-mL bottles, with the first collected before the fuel switch and the last collected once DCN predictions stabilized. IQT values for these samples, indicated by red stars in the plot, aligned with predictions from the fuel sensors. Note that each 50-mL sample took approximately 50 seconds to collect; the time locations for these IQT values were the midpoints of the sample collection time intervals. Averaged DCN predictions output by the sensors during sample collection are shown in Table 5, with errors below 4%. In addition, prediction behaviors during the first and last fuel switches were consistent, highlighting the repeatability of DCN predictions.

In summary, the demonstration showcased the ability of fuel sensors to be integrated in

line with the engine and provide continuous and accurate DCN predictions during fuel switch transitions, validated by IQT measurements of collected samples. Despite not having the fuel included in the training set, the ML models were able to accurately predict the DCN of the DCN34 fuel. This demonstration is, to our knowledge, the first to integrate spectroscopic fuel sensors in line with an engine to showcase the capabilities of real-time measurements of engine-supply fuels.

4. SUMMARY AND FUTURE WORK

To enable on-board fuel property sensing for multi-fuel capable engine control in UAS, various spectroscopic techniques have been investigated and three prototype technologies demonstrated. A comprehensive hydrocarbon dataset was created that resembled jet fuels to train the ML models. All techniques had good performance in predicting DCN with high training and testing scores. These prototype sensors (dispersive NIR, Raman, FT-ATR) were used in an experimental setup to demonstrate real-time fuel property prediction in line with an IC engine. All three sensors were able predict DCNs within the 10% error throughout the demonstration.

For ground vehicle applications, it is vital to incorporate gasoline-based fuels and blends. Recent in-house GCxGC analysis of gasoline has quantified the OH group, and the varied ranges of aromatic groups, setting it apart from diesel- and kerosene-based fuels. Different functional groups, particularly the different ranges of groups, can influence the performance of spectroscopic fuel sensors, particularly if the sensors are not trained on a database inclusive of these groups. Future work involves the expansion of our database to incorporate a comprehensive set of functional groups, enhancing sensing capabilities, as well as expanding sensing capabilities to other fuel properties.

In previous work, a unified evaluation criteria were proposed for spectroscopic fuel sensors for UAS applications [3]. The evaluation criteria consisted of resilience to outliers in DCN predictions and deemed it to be critical for aircraft applications. This may not be the case for ground vehicle applications but should still be evaluated using a challenge set [3]. Furthermore, the resilience criteria encompass temperature and vibration considerations to ensure the sensor is capable of operating within the desired accuracy under deployed conditions. Additionally, the physical criteria-weighting acknowledges the varying importance of SWAP parameters. All these criteria can be tailored to better represent the needs and requirements for ground vehicles, and criteria may need to be added or removed.

5. ACKNOWLEGEMENTS

This research was sponsored by the Army Research Laboratory and performed under Cooperative Agreement Number W911NF-20–2-0223 at UIC and W911NF-20-2-0181 at UW. The research was conducted in collaboration with ARL's Versatile, Tactical Power and Propulsion Essential Research Program (VICTOR ERP), for which Dr. Mike Kweon is the program manager and Dr. Jacob Temme is the deputy program manager. The views and conclusions contained in this document are those of the authors and should not be interpreted as representing the official policies, either expressed or implied, of the Army Research Laboratory or the U.S. Government.

6. REFERENCES

[1] J. P. Stucker, J. F. Schank, and B. Dombey-Moore, *Assessment of DoD Fuel Standardization Policies*. Santa Monica, CA: RAND Corporation, 1994.

[2] J. T. Edwards, "Jet fuel properties," *Report No.(Air Force Research Laboratory Wright-Patterson AFB, 2020), available at https://apps. dtic. mil/sti/citations/AD1093317*, 2020.

[3] A. Abraham *et al.*, "Characteristics of Onboard Sensors for Fuel Ignition Performance," in *AIAA SCITECH 2024 Forum*. doi: 10.2514/6.2024-1244.

[4] M. Tomar *et al.*, "Chapter 16 - Bio-derived sustainable aviation fuels—On the verge of powering our future," in *Developments in Physical & Theoretical Chemistry*, K. B. T.-C. C. and the C. N. F. Brezinsky, Ed., Elsevier, 2023, pp. 521–598. doi: 10.1016/B978-0-323-99213-8.00013-8.

[5] O. J. Hadaller and J. M. Johnson, "World fuel sampling program," *Alpharetta: Coordinating Research Council*, 2006.

[6] K. Craig *et al.*, "SAF Grand Challenge Roadmap Flight Plan for Sustainable Aviation Fuel," 2022.

[7] J. Holladay, Z. Abdullah, and J. Heyne, "Sustainable Aviation Fuel: Review of Technical Pathways Report," 2020.

[8] ASTM, "D975, Standard Specification for Diesel Fuel Oils".

[9] I. ASTM, "Standard Test Method for Cetane Number of Diesel Fuel Oil," *ASTM International: West Conshohocken, PA*, 2019.

[10] I. ASTM, "Standard Test Method for Determination of Ignition Delay and Derived Cetane Number (DCN) of Diesel Fuel Oils by Combustion in a Constant Volume Chamber," *ASTM International: West Conshohocken, PA*, 2018.

[11] A. Sutar *et al.*, "Prospects for Low-Resolution NDIR Sensors to Discern Ignition Properties of Fuels," *J Eng Gas Turbine Power*, vol. 146, no. 7, Feb. 2024, doi: 10.1115/1.4064334.

[12] A. Dalmiya, M. Sheyyab, J. M. Mehta, K. Brezinsky, and P. T. Lynch, "Derived cetane number prediction of jet fuels and their functional group surrogates using liquid phase infrared absorption," *Proceedings of the Combustion Institute*, vol. 000, pp. 1–10, 2022, doi: 10.1016/j.proci.2022.08.104.

[13] D. Ambre, M. Sheyyab, P. Lynch, E. K. Mayhew, and K. Brezinsky, "A Raman spectroscopy based chemometric approach to predict the derived cetane number of hydrocarbon jet fuels and their mixtures," *Talanta*, 2023.

[14] A. Dalmiya, M. Sheyyab, E. K. Mayhew, K. Brezinsky, and P. T. Lynch, "Comparison of Infrared Spectroscopic Methods in Predicting DCN of Jet Fuels and Their Blends Using Chemometric Tools," in *Volume 4: Controls, Diagnostics, and Instrumentation*, American Society of Mechanical Engineers, Jun. 2023, pp. 1–9. doi: 10.1115/GT2023-104099.

[15] P. A. Muzzell, N. C. Johnson, E. R. Sattler, N. Hubble, and L. A. Villahermosa, "U.S. Army Qualification of Alternative Fuels Specified in MIL-DTL-83133H for Ground Systems Use Final Qualification Report: JP-8 Containing Synthetic Paraffinic Kerosene Manufactured Via Fischer-Tropsch Synthesis or Hydroprocessed Esters and Fatty Acids TARDEC Fuels and Lubricants Technology Team," 2013.

[16] E. R. A. Cuellar, D. Rothamer, K. Kim, and C.-B. Kweon, "Optical Engine Study of Variable Energy Assisted Compression Ignition using a Glow Plug for Unmanned Aircraft Propulsion Systems," in *AIAA Scitech 2020 Forum*. doi: 10.2514/6.2020-2281.

[17] N. Miganakallu, J. Stafford, E. Amezcua, K. S. Kim, C.-B. M. Kweon, and D. A. Rothamer, "Impact of Ignition Assistant on Combustion of Cetane 30 and 35 Jet-Fuel Blends in a Compression-Ignition Engine at Moderate Load and Speed," *J Eng Gas Turbine Power*, vol. 145, no. 7, Jul. 2023, doi: 10.1115/1.4062419.

[18] N. Bezaire, K. Wadumesthrige, K. Y. Simon Ng, and S. O. Salley, "Limitations of the use of cetane index for alternative compression ignition engine fuels," *Fuel*, vol. 89, no. 12, pp. 3807–3813, 2010, doi: https://doi.org/10.1016/j.fuel.2010.07.013.

[19] B. P. Vempatapu and P. K. Kanaujia, "Monitoring petroleum fuel adulteration: A review of analytical methods," *TrAC Trends in Analytical Chemistry*, vol. 92, pp. 1–11, Jul. 2017, doi: 10.1016/j.trac.2017.04.011.

[20] J. M. Mehta, P. T. Lynch, E. K. Mayhew, and K. Brezinsky, "Evaluation of Chemical Functional Group Composition of Jet Fuels Using Two-Dimensional Gas Chromatography," *Energy and Fuels*, vol. 37, no. 3, pp. 2294–2306, Feb. 2023, doi: 10.1021/acs.energyfuels.2c03514.

[21] M. Sheyyab, P. T. Lynch, E. K. Mayhew, and K. Brezinsky, "Optimized Synthetic Data and Semi-supervised Learning for Derived Cetane Number Prediction," *Submitted to Fuel*, 2023.

[22] H. Okada and S. T. Sanders, "First-Order Prediction of the Relative Performance of Infrared (IR) Absorption, Raman, and Combined (IR + Raman) Spectroscopy for Estimating Composition and Bulk Properties of Fuel Mixtures," *IEEE Sens J*, vol. 22, no. 16, pp. 16046–16054, 2022, doi: 10.1109/JSEN.2022.3189241.

[23] F. Pedregosa *et al.*, "Scikit-learn: Machine Learning in Python," 2011. [Online]. Available: http://scikit-learn.sourceforge.net.

[24] J. Stafford, E. Amezcua, N. Miganakallu Narasimhamurthy, K. Kim, C. B. Kweon, and D. Rothamer, "Combined Impacts of Engine Speed and Fuel Reactivity on Energy-Assisted Compression-Ignition Operation with Sustainable Aviation Fuels," in *SAE Technical Papers*, SAE International, Apr. 2023. doi: 10.4271/2023-01-0263.

[25] J. Stafford, E. Amezcua, N. Miganakallu Narasimhamurthy, K. Kim, C.-B. Kweon, and D. Rothamer, "Impact of a split-injection strategy on energy-assisted compression-ignition combustion with low cetane number sustainable aviation fuels," in *WCX SAE World Congress Experience*, SAE International, Apr. 2024.

[26] N. Miganakallu, J. Stafford, E. Amezcua, K. S. Kim, C. B. M. Kweon, and D. A. Rothamer, "Impact of Ignition Assistant on Combustion of Cetane 30 and 35 Jet-Fuel Blends in a Compression-Ignition Engine at Moderate Load and Speed," *J Eng Gas Turbine Power*, vol. 145, no. 7, Jul. 2023, doi: 10.1115/1.4062419.